

1500-fold Tunneling Anisotropic Magnetoresistance in a (Ga,Mn)As stack

C. Rüster,¹ C. Gould,¹ T. Jungwirth,^{2,3} J. Sinova,⁴ G. M. Schott,¹
R. Giraud,¹ K. Brunner,¹ G. Schmidt,¹ and L.W. Molenkamp¹

¹Physikalisches Institut (EP3), Universität Würzburg, Am Hubland, D-97074 Würzburg, Germany

²Institute of Physics ASCR, Cukrovarnick 10, 162 53 Praha 6, Czech Republic

³School of Physics and Astronomy, University of Nottingham, Nottingham NG7 2RD, UK

⁴Department of Physics, Texas A&M University, College Station, TX 77843-4242, USA

(Dated: June 24, 2018)

We report the discovery of a super-giant tunneling anisotropic magnetoresistance in an epitaxially grown (Ga,Mn)As/GaAs/(Ga,Mn)As structure. The effect arises from a strong dependence of the electronic structure of ferromagnetic semiconductors on the magnetization orientation rather than from a parallel or antiparallel alignment of the contacts. The key novel spintronics features of this effect are: (i) *both* normal and inverted spin-valve like signals; (ii) a large non-hysteretic magnetoresistance for magnetic fields perpendicular to the interfaces; (iii) magnetization orientations for extremal resistance are, in general, not aligned with the magnetic easy and hard axis. (iv) Enormous amplification of the effect at low bias and temperatures.

PACS numbers: 75.50.Pp, 85.75.Mm

The emerging field of semiconductor based spintronics, which explores the spin and charge degrees of freedom on an equal footing, is expected to lead to novel information technologies that will overcome current key obstacles in the microelectronics roadmap [1]. A main component needed to realize the full potential of this technology is a device with similar behavior as current metal-based spin-valves [2], *and* with novel spintronics features unattainable in their metal counterparts. Previous attempts in this direction have yielded promising spin-valve results [3] apparently mimicking the functionality of the metal devices. However, our recent discovery of tunneling anisotropic magnetoresistance (TAMR) in a single (Ga,Mn)As layer structure [4] suggests that the moderate magnetoresistance (MR) effects observed so far in structures such as the one in Ref. 3 may originate from TAMR rather than the traditional metal tunneling MR (TMR). If this is the case, the device behavior should be much richer than for TMR, and could offer many new functionalities not possible in metal based devices. To investigate this hypothesis, we have fashioned a tunnel structure based on the ferromagnetic semiconductor (Ga,Mn)As. We report the existence of a huge TAMR effect exceeding 100 000% in these structures.

The full layer structure of our device, shown in Fig. 1a, consists of a Ga_{0.94}Mn_{0.06}As (10 nm)/GaAs (2 nm)/Ga_{0.94}Mn_{0.06}As (100 nm) trilayer grown by low temperature molecular beam epitaxy (LT-MBE) on a semi-insulating GaAs substrate and an undoped GaAs buffer layer. The (Ga,Mn)As layers are intrinsically highly p-type due to the Mn and have metallic transport character. The undoped LT-GaAs layer on the other hand is insulating and forms an epitaxial tunnel barrier between the two ferromagnetic layers. The ferromagnetic transition temperature of the (Ga,Mn)As is ~ 65 K.

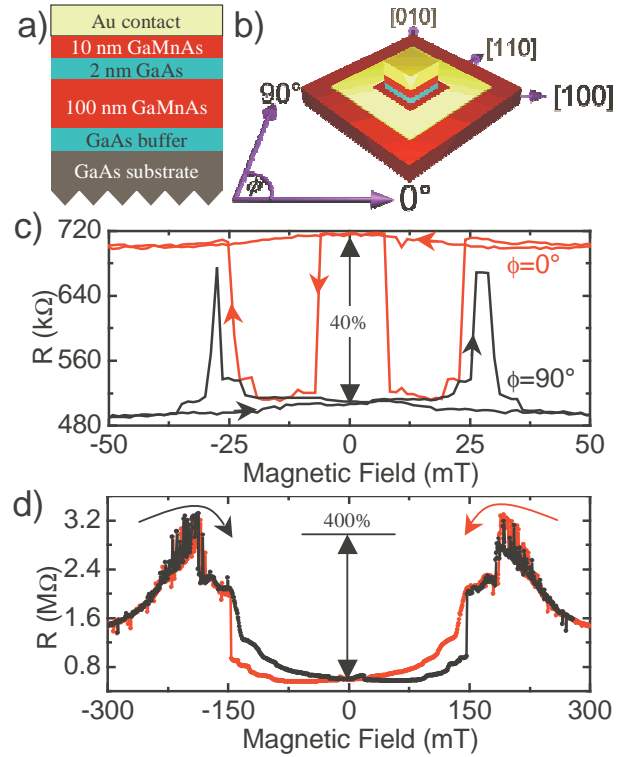


FIG. 1: a) Layer stack and b) sample layout. c) Magnetoresistance near each in-plane easy axis showing both positive and negative 40% effects. d) Magnetoresistance in perpendicular field showing a 400% predominantly non-hysteretic signal.

A schematic of the patterned device is shown in Fig. 1b. Using optical lithography with positive photoresist followed by metal evaporation, lift-off, and wet etching the heterostructure was patterned into a square mesa with sides of 100 μm and a surrounding electrical back contact. Contact to the square mesa is established by an in-situ Ti/Au deposition, whereas the back contact is made

after patterning by depositing Ti/Au onto the lower (Ga,Mn)As layer. Two-probe MR measurements are then performed for current flowing vertically through the layer stack. Since the bulk resistivity of the (Ga,Mn)As is only $\sim 10^{-3} \Omega\text{cm}$, the device resistance is dominated by the tunnel barrier. Identically patterned control samples without a tunnel barrier have a resistance of 10Ω , proving that any bulk (Ga,Mn)As MR is fully negligible.

Transport measurements were carried out in a magnetocryostat fitted with a variable temperature insert and three sets of mutually orthogonal Helmholtz coils allowing the application of magnetic fields \mathbf{H} of up to 300 mT in any direction. Fields applied in the plane of the layers are denoted by their angle ϕ with respect to the [100] crystallographic direction. Two different types of \mathbf{H} scans will be presented: MR-scans, which consist of saturating the sample magnetization in a negative magnetic field along a given direction and then measuring the resistance of the device as $|\mathbf{H}|$ is swept to positive saturation and back again; and ϕ -scans, where the resistance is measured for constant $|\mathbf{H}|$ while sweeping ϕ .

Fig. 1c shows MR-scans taken with a bias voltage $V_B = 10$ mV at a temperature $T = 4.2$ K along $\phi = 0^\circ$ (red) and 90° (black), near the two cubic magnetic easy axes in the (Ga,Mn)As ([100] and [010] respectively) as verified by SQUID. At low $|\mathbf{H}|$ after crossing zero in either sweep directions, \mathbf{M} abruptly reverses its direction. This manifests itself in transport as a discontinuous change in resistance leading to a 40% spin-valve signal. The measurement along 90° appears similar to previous observations [3], and could easily be mistaken for traditional TMR. However, the remarkable sign change observed at $\phi=0^\circ$ points to a different origin of the effect, and strongly suggests an interpretation in line with our previous observations of TAMR in single-ferromagnet devices [4].

As we apply $|\mathbf{H}|$ at other angles in the plane, the amplitude of the effect remains constant whereas the position and sign of the sharp switching events displays a strong angular dependence, with an underlying symmetry consistent with the one reported for a single magnetic layer device [4]. Neglecting some fine structure in the shape of the peaks, the relatively straightforward picture of the two step magnetization reversal reported in [4] accounts for this low $|\mathbf{H}|$ symmetry. It comes from a combination of the magnetic anisotropy of the (Ga,Mn)As, which is principally cubic with a small in-plane uniaxial contribution, and the fact that magnetic reversal takes place via 90° domain wall nucleation and propagation. At low fields, rather than a coherent rotation of the magnetization, the dominating reversal mechanism consists of the magnetization switching abruptly whenever the energy gain by doing so is greater than the energy needed to nucleate/propagate a domain wall. This leads to the symmetry of the magnetization reversal consistent with previous studies in epitaxial Fe layers [5].

Another observation distinguishing our effect from

TMR is a strong MR signal observed when \mathbf{H} is applied perpendicular to the plane of the sample, i.e., along the magnetic hard axis. Fig. 1d shows such a MR-scan at $T = 4.2$ K and $V_B = 5$ mV. The TAMR in Fig. 1d is $\sim 400\%$, much larger than for \mathbf{H} in-plane under similar conditions. As explained in the theory section, we attribute this to a significant growth direction strain in our (Ga,Mn)As layers that induces a large anisotropy between the [001] and [100] (or [010]) directions, compared to the relatively weak in-plane uniaxial anisotropy mentioned above. Note also that the perpendicular TAMR is no longer hysteretic, but occurs on both sides of $\mathbf{H}=0$, indicating that it must be related to the absolute rather than the relative orientations of the ferromagnetic layers.

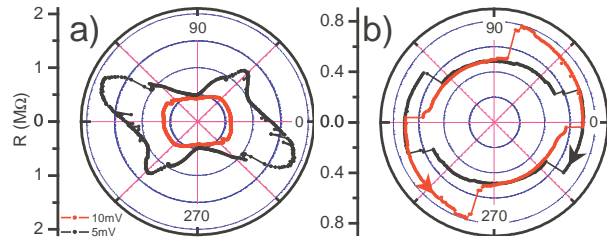


FIG. 2: ϕ -scans at 4.2 K a) in a saturation magnetic field $|\mathbf{H}| = 300$ mT, and b) $V_B = 5$ mV at $|\mathbf{H}| = 25$ mT, just sufficient to switch \mathbf{M} between easy axes.

The TAMR is further evidenced through ϕ -scans at higher magnetic fields. As can already be seen in Fig. 1c, the resistance at saturation is dependent on the direction of magnetization, varying from 480 to 700 k Ω as \mathbf{M} changes from along [010] to [100]. This is a unique characteristic of our device, since in contrast to regular TMR which depends only on the relative orientation of \mathbf{M} in the two layers, our sample is sensitive to the absolute directions of \mathbf{M} in the layers. Therefore it can act as a sensor of the absolute direction of \mathbf{H} . This characteristic is exhibited in the 5 mV, $|\mathbf{H}| = 300$ mT ϕ -scan of Fig. 2a. The measurement is identical for clockwise or counter clockwise ϕ sweeps as $|\mathbf{H}|$ is sufficiently large to saturate \mathbf{M} such that $\mathbf{M} \propto \mathbf{H}$. The resistance changes by more than 250% between its minimum at 90° and its maximum at 165° . The fact that the maximum resistance does not lie along the main crystal and anisotropy axes will be addressed below.

We turn now our attention to Fig. 2b, showing that the ϕ -scan changes dramatically with $|\mathbf{H}|$. Here $|\mathbf{H}| = 25$ mT was chosen to be slightly above the biggest coercive field in the sample such that it can switch \mathbf{M} from one easy axis to the other as ϕ is swept. The sample was prepared in a known state by saturating \mathbf{M} along the uniaxial easy axis (90°) and $|\mathbf{H}|$ was then lowered to 25 mT. After this ϕ was swept in the clockwise (black) or counter clockwise (red curve) direction.

The main features of the data are $\sim 40\%$ jumps in the resistance between the 500 and 700 k Ω levels. These can be understood rather simply by noting that at $\phi = 90^\circ$

the sample is in a low resistance state associated with \mathbf{M} being along the [010] easy axis. As ϕ is swept nearer to the [100] easy axis, \mathbf{M} will eventually switch to this direction, corresponding to a high resistance state due to the additional uniaxial field that breaks the in-plane cubic symmetry in the (Ga,Mn)As layers. The curves must be different for the two sweep directions as they should have approximate mirror symmetry about the easy axis. The deviations from this symmetry may be attributed to non-uniform strain distributions.

A few additional levels are seen in the data on the edges of the large switching events. These intermediate states can be explained in a straightforward way. By design, the magnetic anisotropies of the two layers are not identical as different strain conditions and thicknesses create different coercive fields. Thus, as \mathbf{H} is rotated, the layers do not switch simultaneously, but the softer layer switches earlier. This creates configurations where the magnetizations of the two layers are not collinear, but perpendicular to each other. As a control experiment, a similar ϕ -scan at $|\mathbf{H}| = 15$ mT was made. As expected, since 15 mT is just below the smallest coercive field in the structure, no switching took place, and the resistance of the sample remained constant at its lowest value. This behavior suggests design perspectives for spin valves programmable in rotating magnetic fields above a certain threshold magnitude, but not below.

The data in Figs. 1 and 2 establish unambiguously the TAMR nature of the measured effect. Anisotropies in the (Ga,Mn)As density of states (DOS) with respect to \mathbf{M} , which result from the strong spin-orbit coupling in the ferromagnetic semiconductor valance band, are large enough to explain the effect [4]. Consistently, a sizable anisotropy of the MR of (Ga,Mn)As-based tunnelling structures, comparing the magnetization parallel or perpendicular to the tunneling current, was found in an independent theoretical work employing the Landauer transport formalism [6]. The DOS anisotropy calculations in Ref.4, based on the kinetic-exchange model coupling of valance band holes and polarized Mn local moments, have explained the change of the sign of the TAMR spin-valve like signal with field angle and temperature, and predicted strong enhancement of the effect in epitaxial tunnel junctions characterized by a larger degree of in-plane momentum conservation. Our present study confirms this prediction and some of the new experimental features of the (Ga,Mn)As/GaAs/(Ga,Mn)As TAMR can also be understood based on the DOS anisotropy.

The relative DOS anisotropies, $\Delta\text{DOS}_{int}/\text{DOS}_{int}$, for the DOS at the Fermi energy E_F , integrated over an assumed range of momenta k_z along the tunnelling direction and summed over the occupied spin-split valance bands, are plotted in Fig. 3 for several in-plane magnetization orientations. Note that states at E_F with the largest k_z are expected to have the largest tunnelling probability when in-plane momentum is conserved and,

therefore, increasing the range of k_z contributing to the tunnelling DOS corresponds to relaxing the in-plane momentum conservation condition, or increasing the tunnel barrier transparency. Theoretical curves in panels (a), (b), and (c) were obtained for hole densities 0.1, 0.5, and $1 \times 10^{20} \text{ cm}^{-3}$, respectively. Although the bulk hole densities in our (Ga,Mn)As layers are of order 10^{20} cm^{-3} , a significant depletion is expected in the region near the (Ga,Mn)As/GaAs interface with hole concentration closer to those in panels (b) or (a). The substitutional Mn_{Ga} concentration of 4% considered in the calculations is consistent with the nominal total Mn doping in our (Ga,Mn)As layers. A uniaxial strain along [010] was introduced to model the broken in-plane cubic symmetry in the (Ga,Mn)As.

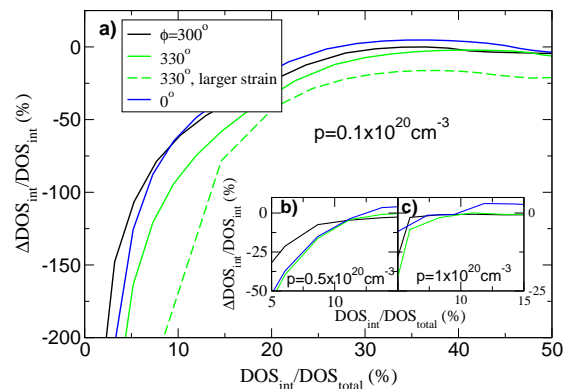


FIG. 3: Theoretical diagrams obtained for hole densities 0.1 (a), 0.5 (b), and $1 \times 10^{20} \text{ cm}^{-3}$ (c) showing the relative difference between the integrated DOS at the Fermi energy for \mathbf{M} along $\phi = 270^\circ$ and three different angles ϕ . The x-axis represents the integrated DOS at the Fermi energy that is assumed to contribute to tunneling, relative to the total DOS at the Fermi energy. Solid (dashed) lines were obtained for a uniaxial strain along [010] direction of 0.2% (0.4%).

Fig. 3 demonstrates that the magnitude of the DOS_{int} anisotropy as well as the magnetization orientations corresponding to extremal tunnelling DOS have a complex dependence on the magnetic tunnel junction parameters. Data in panel (a), e.g., show DOS_{int} anisotropies exceeding 100% for $\text{DOS}_{int}/\text{DOS}_{total} \sim 10\%$. (DOS_{total} denotes the total DOS at E_F .) Here the minimum DOS_{int} is for \mathbf{M} at $\phi = 270^\circ$ while the maximum DOS_{int} is at $\phi = 330^\circ$, i.e., off the main crystal and magnetic anisotropy axis. The result provides an explanation for the distorted cubic symmetry observed in the experimental in-plane angle dependence of the TAMR (see Fig. 2a). The enhanced DOS anisotropy shown by the dashed line in the main panel, which was obtained for larger strain value (larger magnetic anisotropy), is consistent with the experimentally observed enhancement of the TAMR when magnetization is switched between the

easy- and hard-axis (see Fig. 1). We emphasize, however, that the theoretical data in Fig. 3 are only illustrative; a more quantitative comparison between the experiment and theory requires a detailed characterization of the experimental tunnel junction parameters and a systematic theoretical analysis of the TAMR and TMR contributions to the hole transmission coefficients, which is beyond the scope of this short communication and will be published elsewhere.

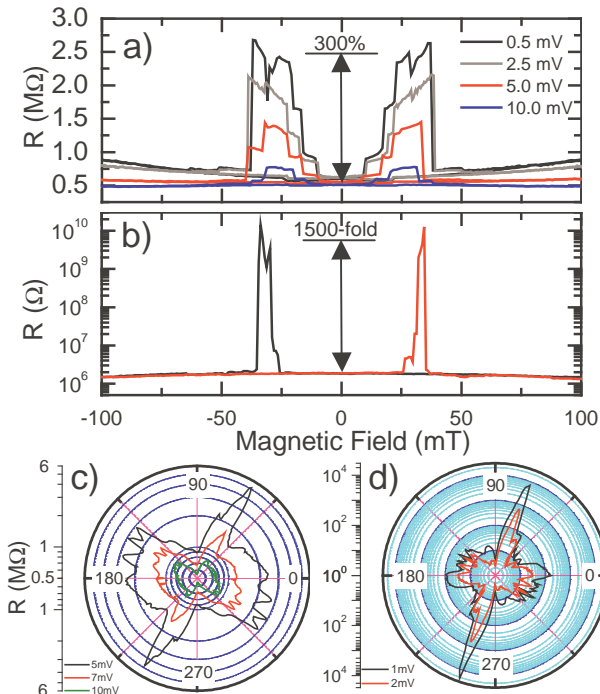


FIG. 4: Amplification of the effect at low bias voltage and temperatures. a) TAMR along $\phi = 65^\circ$ at 4.2 K for various bias voltages. b) Super-giant TAMR at 1.7 K and 1 mV bias. c) and d) ϕ at various bias at 1.7 K showing that at low bias and temperatures, TAMR probes the detailed anisotropies of the density of states.

Another prominent characteristic of our device is the very strong V_B dependence of the signal displayed in Fig. 4a. The various curves show the MR along $\phi = 65^\circ$ at $T = 4.2$ K with V_B ranging from 500 μ V up to 10 mV. The low resistance state has a relatively small variation of $\sim 20\%$ with decreasing bias. In contrast, the high resistance state increases by more than 250%. The amplitude of the TAMR effect is also very sensitive to T , as shown in Fig. 4b. Here we show a $V_B = 1$ mV curve at 1.7 K where the effect has grown to 150 000%. Indeed, this is merely a lower limit corresponding to the detection limit of our current amplifier. Although the amplitude of the effect increases dramatically at low V_B and T , the general symmetry remains unchanged indicating that the origin of the effect is unchanged, but that it is amplified by an additional mechanism.

This super-giant amplification of the TAMR can be

understood as a manifestation of a well known zero bias anomaly [7] in tunneling from a dirty metal which appears due to the opening of an Efros-Shklovskii gap [8] at E_F when crossing the metal-insulator transition. Indeed, such an effect should be observed in our device given the short (Ga,Mn)As mean free path of a few \AA which limits the injector region to a very thin layer near the barrier. Depletion near the barrier must therefore cause a lower carrier density in the injector region than in the bulk of the (Ga,Mn)As slab. The injector will therefore be much closer to the metal-insulator transition than a typical (Ga,Mn)As layer. Moreover, we already know that the DOS changes with M . Therefore, when we perform experiments at low V_B and T , the effective DOS participating in the tunneling can be brought through the metal-insulator transition with reorientation of M , leading to a large amplification of the TAMR effect. A further indication that the Efros-Shklovskii gap is the dominant enhancing mechanism is that the amplification of the effect as T changes from 4.2 to 1.7 K is strong for low bias voltage (1 mV), but disappears at higher voltages (10 mV), consistent with tunneling experiments near the metal-insulator transition of Si:B [7]. Other possible mechanisms for the enhancement of the TAMR, such as disorder and impurity mediated tunneling, may also play a role and should not be summarily dismissed. Further experimental and theoretical study of the problem is needed before the amplification mechanism can be claimed to be fully understood.

Finally, in Fig. 4c and d we present ϕ -scans at 1.7 K for various V_B , which demonstrate another important characteristic of our device which is that it acts as a detector for the anisotropies in the DOS of the (Ga,Mn)As layer. Fig. 4c already shows some fine structure, which becomes much more pronounced at lower the bias. This is to be expected since we start detecting fine structure in the anisotropy of the DOS, which should be complex given that the opening of the gap should develop differently for the various bands which have different effective masses.

In summary, we have observed a super-giant TAMR effect in a (Ga,Mn)As/GaAs/(Ga,Mn)As tunnel structure which can be of order of a few hundred % at 4K, and can be amplified to 150 000% at lower temperatures. The behavior of the structure not only mimics normal TMR when the field is applied along the [010] direction, but also exhibits new functionalities such as a sensitivity to not only the amplitude, but also to the direction of an applied magnetic field. While many of the experimental features of this novel effect can be understood through the one-particle tunneling DOS anisotropies with respect to the magnetization orientation, the dramatic amplification at low biases and temperatures poses new challenging questions for the theory of tunneling transport in disordered interacting electronic systems with strong spin-orbit interaction.

The authors thank A.H. MacDonald and M. Flatté

for useful discussions and V. Hock for sample preparation, and acknowledge financial support from the EU (SPINOSA), the German BMBF (13N8284) and DFG (BR1960/2-2), the Czech Republic GACR (202/02/0912), and the DARPA SpinS program. R.G. thanks the Humboldt foundation for financial support.

-
- [1] Semiconductor Industry Association, "*International Technology Roadmap for Semiconductors*" 2003 edn. <http://public.itrs.net/Files/2003ITRS/Home2003.htm>.
- [2] J. S. Moodera, L. R. Kinder, T. M. Wong, R. Meservey, Phys. Rev. Lett. 74, 3273 (1995)
- [3] Y. Higo, H. Shimizu and M. Tanaka, J. Appl. Phys. 89, 6745, (2001), D. Chiba, F. Matsukura, H. Ohno, PHYSICA E 21, 966, (2004)
- [4] C. Gould, C. Rüster, T. Jungwirth, E. Girgis, G.M. Schott, R. Giraud, G. Schmidt and L.W. Molenkamp, accepted for publication in Phys. Rev. Lett., cond-mat/0407735.
- [5] R.P. Cowburn, S. J. Gray, J. Ferré, J.A.C. Bland, J. Miltat, J. Appl. Phys. 78, 7210 (1995)
- [6] L. Brey, C. Tejedor, J. Fernández-Rossier, cond-mat/045473.
- [7] M. Lee, J.G. Massey, V.L. Nguyen and B.I. Shklovskii, PRB 60, 1582 (1999).
- [8] A.L. Efros and B.I. Shklovskii, J. Phys C 8, L49 (1975).